

Fabiola N. Agüero
Maria R. Morales
Flavia G. Duran
Bibiana P. Barbero
Luis E. Cadús

Research Article

MnCu/Cordierite Monolith used for Catalytic Combustion of Volatile Organic Compounds

Chemical Technology Research Institute, National University of San Luis, National Council for Scientific and Technological Research, San Luis, Argentina.

A MnCu-mixed oxide catalyst supported on a cordierite monolith was synthesized. The catalyst showed very good stability and high homogeneity and presented an excellent catalytic activity in the combustion of ethyl acetate, *n*-hexane, and its mixture. The total conversion temperature of the mixture was determined by the temperature at which the most difficult molecule was oxidized.

Keywords: Catalytic oxidation, Cordierite, Monolithic catalyst

Received: December 18, 2012; *revised:* April 26, 2013; *accepted:* May 16, 2013

DOI: 10.1002/ceat.201200713

1 Introduction

Volatile organic compounds (VOCs) are an important type of air pollutant which covers a wide range of compounds that differ in their properties and chemistry, but display similar behavior in the atmosphere. These compounds require special attention due to their toxicity, high stability, and persistence in the environment [1–3]. Catalytic oxidation is an effective way for reducing the emissions of VOCs [4]. Platinum and palladium supported on alumina or silica are the most commonly used catalysts for total oxidation [5–9]. The high cost of noble metals has increased the interest in their replacement by transition metal oxides, such as those of Cu, Mn, Co, and Fe, which might satisfy the requirements of the treatment process [10]. In previous papers [11, 12], MnCu-based catalysts, which were synthesized by the coprecipitation method, were studied. It was found that a low amount of Cu in the mixed catalyst was sufficient to obtain a higher catalytic activity than Mn₂O₃. Mn₉Cu₁ catalyst presented the best performance. The synthesis of bulk or supported catalysts in granular form is a well-known process. Recently, monolithic supports have been considered as an alternative geometry to conventional granular catalysts [13, 14]. The advantages of these supports include very low pressure drop, uniform flow distribution within the monolith matrix, and easier accessibility of catalytic active centers of the monolithic walls by the reacting gases. One of the methods used to deposit the active phase on the monolithic supports is coating with a slurry, commonly called *washcoating*. The monolith is dipped in a slurry of catalyst particles of a comparable size to that of the macropores of the support [15]. This method involves the previous synthesis of the catalyst.

The method used to synthesize the Mn₉Cu₁ catalyst developed in earlier works [11, 12] requires the washing of the precipitate for the removal of residual sodium. This implies that a large amount of water has to be treated for a certain quantity of catalyst. In order to obtain a catalyst with excellent catalytic performance in a larger scale, it is necessary to decrease the synthesis steps as well as to minimize the volumes of reagents and solvents used. Thus, an alternative to washcoating is the impregnation method, where the monolith is dipped in a solution of precursor salts containing the active phase.

Industrial exhaust gases are mainly composed of VOC mixtures of different chemical character, such as aromatic hydrocarbons, alkanes, and oxy-derivatives, i.e., alcohols, acetates, and ketones. The catalysts have to be able to treat different kinds of substances together, simultaneously. Under these conditions, it may be difficult to predict the behavior of the catalyst and to control the destruction efficiency, because the mixture effects may be significant and strongly dependent upon the catalyst and mixture composition [16–19].

The scope of this work is to reproduce the excellent catalytic performance of Mn₉Cu₁ powder catalyst in VOC combustion by depositing the active phase on cordierite ceramic monoliths using a simple method in order to favor the subsequent scaling. The catalytic performance in the oxidation of ethyl acetate and *n*-hexane, either separately or in a binary mixture, was evaluated.

2 Experimental

2.1 Synthesis of Catalysts

Cordierite monoliths were provided by Corning (cell density: 400/6.5) and samples of 0.7 cm × 0.7 cm × 3 cm in laboratory scale were used. The samples were blown with air in order to eliminate particles or dust from the packaging. Then, monoliths were dipped in a colloidal alumina slurry (Nyacol®), for 10 s and withdrawn at a constant speed of 3 cm min⁻¹. The ex-

Correspondence: Dr. M. Morales (mrmorale@unsl.edu.ar), Chemical Technology Research Institute, National University of San Luis – National Council for Scientific and Technological Research (CONICET), Mail box 290, San Luis, Argentina.

cess suspension was eliminated by blowing them with air for 45 s. Monoliths were then dried at 120 °C for 1 h. One, two, or three soaks were made and finally, the samples were calcined at 500 °C for 2 h. The monoliths, previously coated with alumina, were impregnated with aqueous solutions of $(\text{CH}_3\text{CO}_2)_2\text{Mn}\times 4\text{H}_2\text{O}$ and $(\text{CH}_3\text{CO}_2)_2\text{Cu}\times 4\text{H}_2\text{O}$ in a 9:1 molar ratio with a total precursor concentration of 0.4 g mL⁻¹. Monoliths were immersed in the solution and agitated by ultrasound for 1 h. The excess solution was removed by blowing them with air for 45 s. Finally, they were dried at 80 °C for 24 h and calcined at 500 °C for 2 h. One or two impregnations were made with a calcination step in-between the impregnations. The monoliths were called xMnCu/Al₂O₃/cordierite where x = 1 or 2, depending on the number of impregnations performed.

2.2 Characterization Techniques

Adherence test

The adherence of the coatings was evaluated in terms of the weight loss after exposure of the monoliths to ultrasounds. Monoliths were immersed in 25 mL petroleum ether inside a sealed beaker and then treated in an ultrasound bath for 30 min. After that, they were dried at 120 °C for 2 h. The weight loss was gravimetrically determined by measuring the weight of the samples, both before and after the ultrasonic treatment.

X-ray diffraction (XRD)

XRD patterns were obtained by using a Rigaku diffractometer operated at 30 kV and 25 mA by employing Cu K α radiation with Nickel filter ($\lambda^1 = 0.15418$ nm).

Textural characteristics measurement

Adsorption–desorption isotherms of nitrogen at 77 K were performed in a Gemini V apparatus from Micromeritics after out-gassing the monoliths at 120 °C. A home-made cell was used for the measurement of complete monoliths.

Scanning Electron Microscopy (SEM)

The morphology of samples was examined with a LEO 1450 VP scanning electron microscope provided with energy dispersive X-ray analysis (EDAX) equipment for the quantitative analysis.

Temperature programmed reduction (TPR)

The TPR was performed in a quartz tubular reactor using a TCD as detector. Samples of 500 mg were used. The reducing gas was a mixture of 5 vol% H₂/N₂ at a total flow rate of 30 mL min⁻¹. The temperature was increased at a rate of 5 °C min⁻¹ from room temperature to 700 °C.

2.3 Catalytic Tests

The monolithic catalysts were evaluated in the combustion of *n*-hexane and ethyl acetate, and its binary mixture. The reacting stream was 300 cm³ min⁻¹, with a composition of 1000 mg_C m⁻³ or 2000 mg_C m⁻³ diluted in synthetic air having a space velocity of 12 000 h⁻¹. The oxidation of two-component mixtures was done using 1000 mg_C m⁻³ of each component. The gaseous mixtures were analyzed by gas chromatography using a Buck Scientific Mod 910 with a FID detector, a methanizer, and a Carbowax 20M/Chromosorb W column.

3 Results and Discussion

3.1 Coating with Alumina

In order to facilitate the adhesion of the active phase to the monolithic structure, a pre-coating of the monolith with a layer of a support was made. This addition not only improves the stability of the catalyst, but may also produces an increase in the surface area [20]. High surface area γ -alumina is one of the most suitable materials for the dispersion of commonly used combustion catalysts. It is normally applied as a uniformly-dispersed thin layer on a ceramic support. Monolith was coated with one, two, or three layers of alumina. The stability of the alumina was tested by means of an adherence test. The results are shown in Tab. 1.

Table 1. S_{BET} , retained alumina, active phase loading, and weight loss of monoliths.

Monolith	S_{BET} [m ²]	Retained loading [mg]	Weight loss [%]
Cordierite	0.5		
1Al ₂ O ₃ /cordierite		58	1.25
2Al ₂ O ₃ /cordierite	20.9	120	0.2
3Al ₂ O ₃ /cordierite		160	2.7
1MnCu		27	1.5*
2MnCu	16	59	1.4*

*Weight loss [%] is calculated considering both active phase and alumina loading.

As it can be observed, a higher alumina loading was obtained after the third immersion; however, a higher adherence was obtained after the second immersion. Thus, monoliths with two alumina coatings were used as supports of the active phase. As it was expected, the S_{BET} of the bare cordierite monolith notably increased with the alumina coating (Fig. 1). The alumina-washcoated monolith was characterized by SEM. Fig. 1 presents SEM micrographs of a bare cordierite monolith. The alumina-coated monolith, after two immersions, is shown in Fig. 2.

The cordierite support is completely covered with alumina. Cross-section micrographs reveal that the alumina layer is

1) List of symbols at the end of the paper.

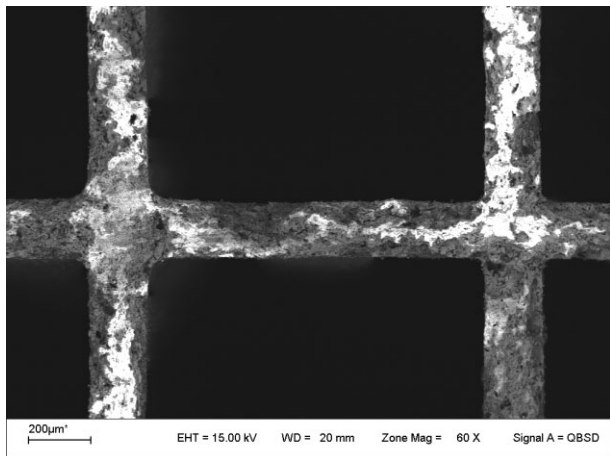


Figure 1. Cross-section SEM micrograph of a bare monolith.

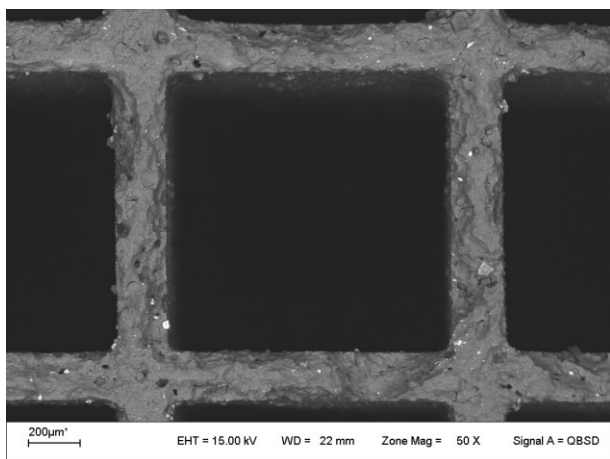


Figure 2. Cross-section SEM micrograph of an alumina covered monolith.

5–10 μm thick on the side of the channels. It is worth mentioning that the thin cracks observed are not due to the calcination steps. They were actually formed during the initial drying step. This was also observed by Villegas et al. [21] on alumina-washcoated monoliths. The small cracks were already present prior to calcination, and did not change upon increasing the temperature up to 800 °C.

3.2 Impregnation of the Monolith with the Active Phase

The impregnation with the active-phase precursor step requires a homogeneous distribution on the surface to avoid accumulating points that favor the growth of crystalline Mn_2O_3 [22]. Therefore, the monolith that had been previously coated with alumina was immersed in the acetate solution and the agitation was carried out in an ultrasound bath, thus preventing probable flow canalizations. Moreover, this method of agitation by ultrasound can be perfectly used for the impreg-

nation of monoliths on a larger scale. One or two successive impregnations were made because it has been demonstrated that a higher number of immersions led to unstable and non-homogeneous catalyst layers [23]. As it is shown in Tab. 1, a higher active-phase loading was obtained with a second impregnation, and the weight loss after adherence test was similar, about 1.5% in all catalysts prepared by this method, indicating a very good adhesion of the active phase and alumina coating. A visual examination of the monolith that has been cut in two parts in the axial direction (Fig. 3) shows homogeneity in the active-phase distribution. This was also observed in a SEM examination (Fig. 4). The active-phase layer is homogeneously deposited over the channel length. Fig. 5 illustrates the element mapping of manganese and copper in the alumina-washcoated catalysts. Both copper and manganese are well dispersed all over the catalyst. Copper is always in lower proportions compared to manganese. In the back-scattered electron (BSE) image of Fig. 6, it can be seen that the active phase penetrates the open macropores of the support at the surface, suggesting a good anchoring onto the support.

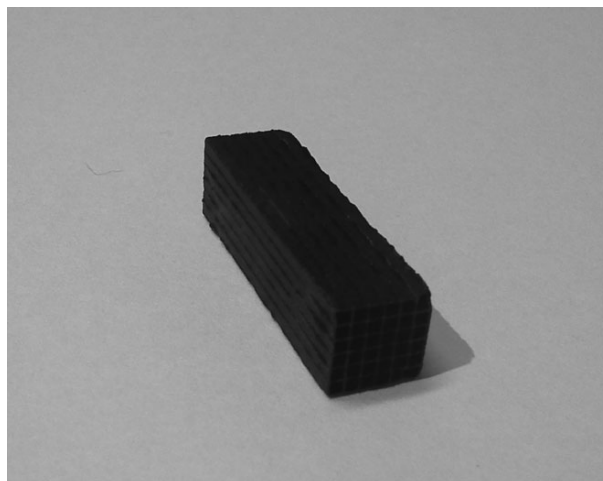


Figure 3. Axial-section view of the MnCu-impregnated monolith.

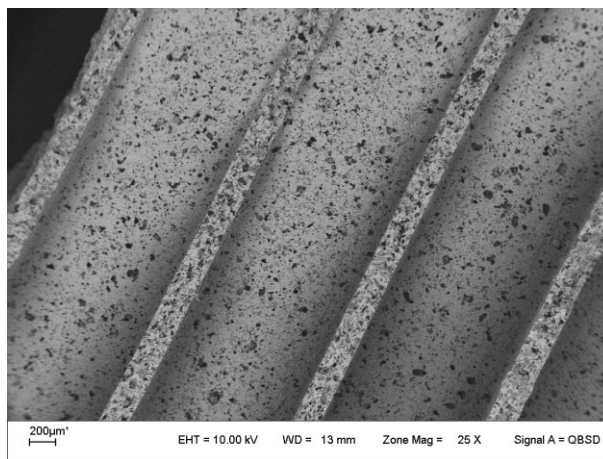


Figure 4. Axial-section SEM micrograph of the MnCu-impregnated monolith.

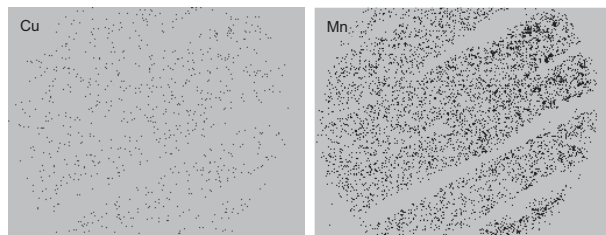


Figure 5. Element mapping of manganese and copper of the MnCu-impregnated monolith.

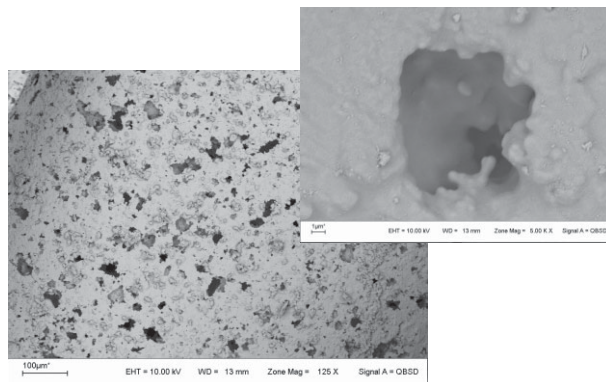


Figure 6. A back-scattered electron (BSE) image of a monolith channel.

The reproducibility of the synthesis method could be estimated by preparing batches of three monoliths with the same characteristics, i.e., the weight gained after two impregnations followed by calcination were similar to a standard deviation lower than 1 %.

In summary, the monolithic catalyst was synthesized using a simple and reproducible method. Minimizing the number of steps and the volume of reagents and solvents used generated a lower amount of waste. Thus, catalysts with homogeneous and well-adhered coatings were obtained. It is important to note that the simplicity of this method in laboratory scale may be used perfectly in a larger scale.

3.3 Characterization of MnCu-coated Monolith

The specific surface area of the MnCu-coated monolith is shown in Tab. 1. When the alumina-coated cordierite monolith was impregnated with the active phase, a slight decrease in S_{BET} was observed. X-ray diffraction technique was used in order to determinate the nature of the active phase deposited on the monolith. The XRD pattern of the bare cordierite presented the peaks corresponding to a cordierite phase (PDF 12-303). The diffractograms of the alumina/cordierite and 2MnCu monoliths did not show differences with respect to the bare monolith, and no peaks corresponding to Al_2O_3 ,

CuO , or Mn_2O_3 were detected. This could be due to a low amount of the active phase below the detection limits of the technique, or to the high dispersion of the active phase on the support. It is well known that highly-dispersed manganese oxide species are obtained using manganese acetate as a precursor of the active phase [24], or using small amounts of CuO [11], as in this case. A very useful tool to obtain information about the distribution of the active phase on the support is temperature-programmed reduction. Fig. 7 shows the reduction profile of the 2MnCu monolithic catalyst, which is compared to the reduction profile of the MnCu powder catalyst studied in a previous paper [11]. Both samples presented a main reduction signal with a maximum at 270 °C, a shoulder at 235 °C, and small signals at about 200 °C. This signal reduction at low temperature could be attributed to highly-dispersed manganese oxide species, thus corroborating the assumptions obtained from XRD results.

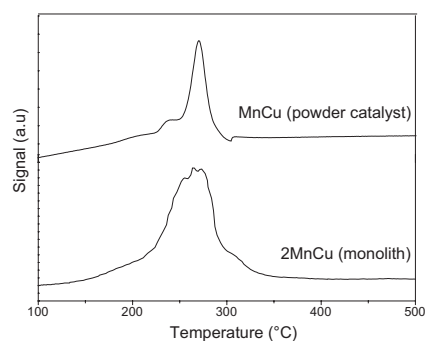


Figure 7. Temperature programmed reduction profiles.

3.4 Catalytic activity

The monolith synthesis can be measured from its catalytic activity in VOC combustion. The 2MnCu catalyst was selected for the catalytic performance studies due to the higher retained active-phase loading and its excellent adherence. The sample was evaluated in total oxidation of ethyl acetate, *n*-hexane, and its binary mixture. The catalytic results are shown in Tab. 2 and Fig. 8.

The monolith showed very good activity in the ethyl acetate combustion. It is worth mentioning that only small amounts of acetaldehyde were detected at low temperatures, besides total oxidation products, CO_2 and H_2O ; however, it was completely oxidized at the same temperature as ethyl acetate. The conversion of ethyl acetate started below 150 °C and it was

Table 2. Catalytic performance in ethyl acetate, *n*-hexane, and its binary mixture.

Ethylacetate (E. A) conversion			Hexane conversion		
VOC	T_{50} [°C]	T_{90} [°C]	VOC	T_{50} [°C]	T_{90} [°C]
1000 E.A.	178	190	1000 Hex	208	240
2000 E.A.	192	198	2000 Hex	213	245
1000 E.A + 1000 Hex	190	198	1000 Hex+1000 E.A.	218	242

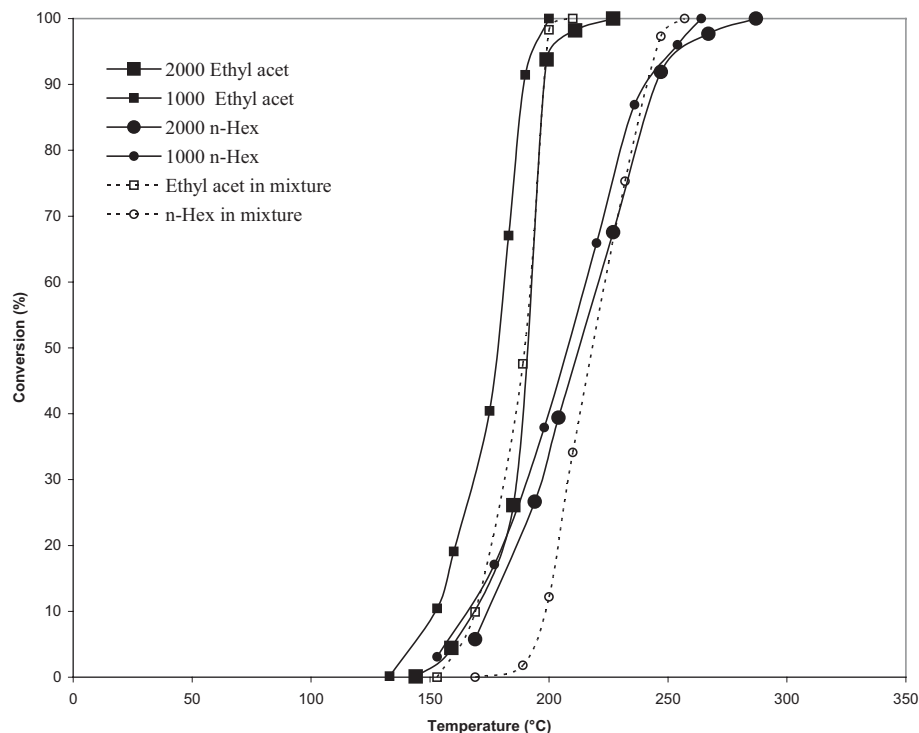


Figure 8. VOCs conversion vs. reaction temperature.

completed below 200 °C, showing a T_{90} value (temperature corresponding to the 90% conversion of VOC) of 190 °C when 1000 $\text{mg}_C \text{m}^{-3}$ was fed. It can be observed that these values increase by about 10 °C as the composition of the VOC in the feed increases; this is expected since the contact time is shorter. The monolith also showed an excellent catalytic activity in *n*-hexane combustion. Only products of total combustion were detected. T_{50} and T_{90} values were around 208 °C and 240 °C, respectively, in the case of 1000 $\text{mg}_C \text{m}^{-3}$, and only a difference of about 5 °C was observed when increasing the composition of the feed. These results are evidence of the excellent catalytic activity of this monolithic catalyst and make it very promising for industrial applications. The comparison of the catalytic activity of this catalyst with those presented in literature is not an easy task since the operating conditions are very different. However, this catalyst is notably more active than our previously-reported catalysts: Mn9Cu1 powder catalyst [11], $\text{MnO}_x/\text{Al}_2\text{O}_3$ supported on metallic monoliths [25,26], and MnCu/FeCr alloy monolith [20]. The comparison may be done taking into account the difficulty in the combustion of the tested molecules. However, there are some cases in literature which presented a similar catalytic performance to our catalyst. For example, Santos et al. [27] reported a T_{90} value of 195 °C, corresponding to the combustion of ethyl acetate in a Cs-Criptomelane catalyst. The major difference with our catalyst is the complexity of the synthesis method used, since the criptomelane phase was obtained using the reflux approach in an acidic medium [28] and Cesium was incorporated into the tunnel structure by ion-exchange. Frias et al. [29] reported the catalytic activity of a criptomelane/AISI 304 monolith, also prepared by the reflux method, in the combustion of ethyl ace-

tate. Lahousse et al. [18] presented a very active MnO_2 catalyst in the combustion of *n*-hexane. This catalyst was not supported in a monolith and was evaluated in the combustion of a low concentration of VOC. Moreover, this catalyst is unstable at high temperatures, which are feasible due to the exothermic character of the reaction, generating possible hot points. Zavyalova et al. [30] published the catalytic behavior of a CoCr catalyst in the combustion of *n*-hexane. Their results were similar to our catalysts; however, the CoCr catalyst was evaluated in a low concentration of VOC. Sanz et al. [31] studied Pt/anodized aluminum foam catalyst in total combustion of toluene. The results of the catalytic performance were excellent; nevertheless, our catalyst, a supported metallic oxide, presented a similar catalytic behavior to this supported, noble-metal catalyst. This fact makes our catalyst very interesting from an economical point of view too.

As real industrial emissions usually contain mixtures of volatile organic compounds, studies of the catalytic activity on a single molecule of VOC partially represent the catalyst application. Therefore, it is interesting to test the catalytic behavior of our monolithic catalyst in the oxidation of VOC mixtures. The mixture of ethyl acetate (oxy-derivative) and *n*-hexane (alkane) was selected in this study because they are compounds of different chemical character. Ethyl acetate conversion obtained during the mixture combustion is lower than that obtained during 1000 $\text{mg}_C \text{m}^{-3}$ ethyl acetate single oxidation; however, the curve is similar to that obtained during 2000 $\text{mg}_C \text{m}^{-3}$ ethyl acetate single oxidation. Thus, ethyl acetate combustion is affected by the presence of another molecule, *n*-hexane in this case, or by the presence of the same molecule as it occurs during 2000 $\text{mg}_C \text{m}^{-3}$ ethyl acetate single oxidation. Considering the *n*-hexane combustion, it can be observed that the conversion of this molecule in a mixture is strongly inhibited at low temperatures under 220 °C, approximately, where there is still unconverted ethyl acetate. Evidently, the presence of ethyl acetate in the mixture slows *n*-hexane oxidation. The same outcome was found by V. Blasin-Aubé et al. [32], since they observed that the presence of ethyl acetate inhibited the rates for *n*-hexane in the mixture oxidation on $\text{La}_{0.8}\text{Sr}_{0.2}\text{MnO}_{3+x}$ perovskite catalyst, and they explained this inhibition as being a result of the competition for the adsorption sites. The component which is preferentially adsorbed is easily oxidized. In this case, ethyl acetate would adsorb strongly on the catalyst surface, as it was observed to behave in a previous paper on the $\text{MnO}_x/\text{Al}_2\text{O}_3$ catalyst [33]. However, at higher temperatures, the *n*-hexane conversion remains similar to that of the single VOC combustion. This is to say that CO_2 and

water (ethyl acetate total combustion products) do not affect *n*-hexane conversion. Indeed, the total conversion temperature of the mixture is determined by the temperature at which the most difficult molecule is oxidized.

4 Conclusions

The monolithic catalyst was synthesized using a simple and reproducible method, minimizing the number of steps and the volume of reagents and solvents used. Catalysts with homogeneous and well-adhered coatings were obtained. Through this simple method, it was possible to reproduce and even improve the properties of powder catalyst, obtaining a monolithic catalyst with excellent catalytic activity in the oxidation of ethyl acetate, *n*-hexane, and their mixture. Total conversion temperature of the mixture was determined by the temperature at which the most difficult molecule was oxidized.

Acknowledgment

The financial support from Universidad Nacional de San Luis (UNSL), Consejo Nacional de Investigaciones Científicas y Técnicas (CONICET), and Agencia Nacional de Promoción Científica y Tecnológica (ANPCyT) of Argentina is gratefully acknowledged.

The authors have declared no conflict of interest.

References

- [1] M. Alifanti, M. Florea, S. Somacescu, V. I. Parvulescu, *Appl. Catal., B* **2005**, *60* (1–2), 33–39. DOI: 10.1016/j.apcatb.2005.02.018
- [2] M. Labaki, J. F. Lamonier, S. Siffert, E. A. Zhilinskaya, A. Aboukai, *Kinet. Catal.* **2004**, *45* (2), 227–233. DOI: 10.1023/B:KICA.0000023796.52228.44
- [3] E. Noordally, J. R. Richmond, S. F. Tahir, *Catal. Today* **1993**, *17* (1–2), 359–366. DOI: 10.1016/0920-5861(93)80039-4
- [4] E. C. Moretti, N. Mukhopadhyay, *Chem. Eng. Prog.* **1993**, *89*, 20.
- [5] H. L. Tidahy, S. Siffert, J. F. Lamonier, E. A. Zhilinskaya, A. Aboukai, Z. Y. Yuan, A. Vantomme, G. De Weireld, *Appl. Catal., A* **2006**, *310*, 61–69. DOI: 10.1016/j.apcata.2006.05.020
- [6] S. K. Ihm, Y. D. Jun, D. C. Kim, K. E. Jeong, *Catal. Today* **2004**, *93*, 149–154. DOI: 10.1016/j.cattod.2004.06.096
- [7] M. J. Patterson, D. E. Angove, N. W. Cant, *Appl. Catal., B* **2000**, *26* (1), 47–57. DOI: 10.1016/S0926-3373(00)00110-7
- [8] J. Tsou, P. Magnoux, M. Guisnet, J. J. M. Orfao, J. L. Figueiredo, *Appl. Catal., B* **2005**, *57* (2), 117–123. DOI: 10.1016/j.apcatb.2004.10.013
- [9] C. M. Manta, G. Bozga, G. Bercau, C. S. Bildea, *Chem. Eng. Technol.* **2012**, *35* (12), 2147–2154. DOI: 10.1002/ceat.201200371
- [10] S. Vigneron, P. Deprelle, J. Hermia, *Catal. Today* **1997**, *27* (1–2), 229–236. DOI: 10.1016/0920-5861(95)00192-127
- [11] M. Morales, B. Barbero, L. Cadús, *Appl. Catal., B* **2006**, *67*, 229–236. DOI: 10.1016/j.apcatb.2006.05.006
- [12] M. Morales, B. Barbero, L. Cadús, *Fuel* **2008**, *87* (7), 1177–1186. DOI: 10.1016/j.fuel.2007.07.015
- [13] I. M. Lachman, J. L. Williams, *Catal. Today* **1992**, *14* (2), 317–329. DOI: 10.1016/0920-5861(92)80032-1
- [14] A. Cybulski, J. Moulijn, *Catal. Rev.: Sci. Eng.* **1994**, *36*, 179–270. DOI: 10.1080/01614949408013925
- [15] A. A. Nijhuis, A. E. W. Beers, T. Vergunst, I. Hoek, F. Kapteijn, J. A. Moulijn, *Catal. Rev.: Sci. Eng.* **2001**, *43*, 345–380.
- [16] J. R. González-Velasco, A. Aranzabal, R. López-Fonseca, R. Ferret, J. A. González-Marcos, *Appl. Catal., B* **2000**, *24* (1), 33–43. DOI: 10.1016/S0926-3373(99)00087-9
- [17] S. K. Gangwal, M. E. Mullins, J. J. Spivey, P. R. Caffrey, B. A. Tichenor, *Appl. Catal.* **1988**, *36*, 231–247. DOI: 10.1016/S0166-9834(00)80118-9
- [18] C. Lahousse, A. Bernier, P. Grange, B. Delmon, P. Papaefthimiou, T. Ioannides, X. Verykios, *J. Catal.* **1998**, *178* (1), 214–225. DOI: 10.1006/jcat.1998.2148.
- [19] A. Musialik-Piotrowska, K. Syczewska, E. Schubert, *Environ. Prot. Eng.* **2000**, *26*, 119–130.
- [20] B. P. Barbero, L. Costa-Almeida, O. Sanz, M. R. Morales, L. E. Cadus, M. Montes, *Chem. Eng. J.* **2008**, *139*, 430–435. DOI: 10.1016/j.cej.2007.12.03
- [21] L. Villegas, F. Masset, N. Guilhaume, *Appl. Catal., A* **2007**, *320*, 43–55. DOI: 10.1016/j.apcata.2006.12.011
- [22] F. Kapteijn, D. van Langeveld, J. A. Moulijn, A. Andreini, M. A. Vuurman, A. M. Turek, J.-M. Jehng, I. E. Wachs, *J. Catal.* **1994**, *150* (1), 94–104. DOI: 10.1006/jcat.1994.1325
- [23] C. Agrafiotis, A. Tsetsekou, *J. Mater. Sci.* **2000**, *35* (4), 951–960. DOI: 10.1023/A:1004762827623.
- [24] F. N. Agüero, A. Scian, B. P. Barbero, L. E. Cadús, *Catal. Today* **2008**, *133–135*, 493–501. DOI: 10.1016/j.cattod.2007.11.044
- [25] F. N. Agüero, B. P. Barbero, L. Costa Almeida, M. Montes, L. E. Cadús, *Chem. Eng. J.* **2011**, *166* (1), 218–223. DOI: 10.1016/j.cej.2010.10.064
- [26] F. N. Agüero, B. P. Barbero, O. Sanz, F. J. Echave Lozano, M. Montes, L. E. Cadús, *Ind. Eng. Chem. Res.* **2010**, *49* (4), 1663–1668. DOI: 10.1021/ie901567a
- [27] V. P. Santos, M. F. R. Pereira, J. J. M. Orfao, J. L. Figueiredo, *Appl. Catal., B* **2009**, *88* (3–4), 550–556. DOI: 10.1016/j.apcatb.2008.10.006
- [28] J. Luo, Q. Zhang, A. Huang, S. L. Suib, *Microporous Mesoporous Mater.* **2000**, *35–36*, 209–217. DOI: 10.1016/S1387-1811(99)00221-8
- [29] D. M. Frías, S. Nousir, I. Barrio, M. Montes, L. M. Martínez T, M. A. Centeno, J. A. Odriozola, *Appl. Catal., A* **2007**, *325* (2), 205–212. DOI: 10.1016/j.apcata.2007.02.038
- [30] U. Zavyalova, B. Nigrovski, K. Pollok, F. Langenhorst, B. Müller, P. Scholz, B. Ondruschka, *Appl. Catal., B* **2008**, *83* (3–4), 221–228. DOI: 10.1016/j.apcatb.2008.02.015
- [31] O. Sanz, F. J. Echave, M. Sanchez, A. Monzón, M. Montes, *Appl. Catal., A* **2008**, *340* (1), 125–132. DOI: 10.1016/j.apcata.2008.02.007
- [32] V. Blasin-Aubé, J. Belkouch, L. Monceaux, *Appl. Catal., B* **2003**, *43* (2), 175–186. DOI: 10.1016/S0926-3373(02)00302-8
- [33] F. N. Agüero, B. P. Barbero, L. Gambaro, L. E. Cadús, *Appl. Catal., B* **2009**, *91* (1–2), 108–112. DOI: 10.1016/j.apcatb.2009.05.012